Advanced ICTs for Disaster Management and Threat Detection:

Collaborative and Distributed Frameworks

Eleana Asimakopoulou
Loughborough University, UK

Nik Bessis
University of Bedfordshire, UK

INFORMATION SCIENCE REFERENCE
Hershey · New York

Editorial Advisory Board

List of Reviewers

Yolanda Barrientos, *Universidad Pedagógica Experimental Libertador, Venezuela*
Svetlana Bayda, *Civil Defense Academy of the Ministry of the Russian Federation, Russia*
Steve Bloomer, *University of Teesside, UK*
Rui Chen, *Ball State University, USA*
Andre Clark, *University of Glamorgan, UK*
Tina Comes, *Karlsruhe Institute of Technology, Germany*
Edouard Dervichian, *Swissphone Telecom AG, Switzerland*
*Angus Duncan, University of Bedfordshire, U*K
Irina Ermakova, *IHNA&NPh RAS, Russia*
Stathes Hadjiefthymiades, *University of Athens, Greece*
Matina Halkia, *Joint Research Centre of the European Commission, Italy*
José G. Hernández R., *Universidad Metropolitana, Venezuela*
Michael Hiete, *Karlsruhe Institute of Technology, Germany*
Pierre Kuonen, *University of Applied Sciences of Western Switzerland, Switzerland*
Sunitha Kuppuswamy, *Anna University Chennai, India*
JinKyu Lee, *Oklahoma State University, USA*
Jens P. Linge, *Joint Research Centre of the European Commission, Italy*
Fuad Mallick, *Bangladesh and Kathmandu University, Nepal*
Ulrich Meissen, *Fraunhofer Institute for Software and Systems Engineering, Germany*
Danielle Mirliss, *Seton Hall University, USA*

Chapter 16
Sensor and Computing Infrastructure for Environmental Risks:
The SCIER System

Odysseas Sekkas
University of Athens, Greece

Dimitrios V. Manatakis
University of Athens, Greece

Elias S. Manolakos
University of Athens, Greece

Stathes Hadjiefthymiades
University of Athens, Greece

ABSTRACT

The SCIER platform is an integrated system of networked sensors and distributed computing facilities, aiming to detect and monitor a hazard, predict its evolution and assist the authorities in crisis management for hazards occurring at Wildlife Urban Interface (WUI) areas. The goal of SCIER is to make the vulnerable WUI zone safer for the citizens and protect their lives and property from environmental risks. To achieve its objective, SCIER integrates technologies such as: (1) wireless sensor networks for the detection and monitoring of disastrous natural hazards, (2) advanced sensor data fusion and management for accurately monitoring the dynamics of multiple interrelated risks, (3) environmental risk models for simulating and predicting the evolution of hazardous phenomena using Grid-computing. In this chapter we present the key software components of the SCIER system architecture, namely the sensor data fusion component and the predictive modeling and simulation component.

DOI: 10.4018/978-1-61520-987-3.ch016

INTRODUCTION

The tendency for the development of extensive WUI (Wildlife Urban Interface) areas is a relatively new phenomenon. This refers to all types of areas where forests, water bodies, and rural lands interface with homes, other buildings and infrastructures, including first and secondary home areas, industrial areas and tourist developments (Stewart, 2007). The related problems that it generated, especially with regards to increasing fire and flood risks, started becoming noticeable only in the 1990s. The rapid development of WUI areas is the result of pollution and overpopulation of city centers that grew in the 1970s. However, in many cases, the rapid development of such WUIs was unplanned, or poorly planned. Settlements were built without efficient road networks, and homes and other buildings were developed in or near areas that form the flood plain of water catchments. Often there is no provision for routes of escape in case of a disaster.

The *Sensing and Computing Infrastructure for Environmental Risks* (SCIER) system constitutes an integrated sensing and computing platform capable of delivering to the authorities and the citizens valuable real time information regarding natural hazards that may affect the WUI. SCIER aims at providing the functionality needed for detecting, monitoring and forecasting the hazard's evolution. Sensors deployed in the region monitor environmental parameters (e.g., temperature, humidity, wind direction and speed) and feed the data to predictive models running in the computing infrastructure. The SCIER platform builds upon existing technical expertise and recent progress in the areas of sensors, communications, Grid computing, Geographical Information Systems (GIS), data fusion and predictive modeling. Indeed, the information produced by the SCIER platform can in many cases be a key factor in the effective fighting of the hazard's consequences. SCIER predicts the evolution of the main phenomenon as well as the risks associated with any secondary phenomena it may trigger. Furthermore, for the people living in vulnerable WUI areas, it addresses their needs for security and reliable alerting services. Finally, SCIER provides Civil Protection Authorities with a tool for the effective management of crisis situations caused by natural hazards.

Related Work

In this section we briefly discuss prior research activities on natural hazard detection and monitoring. Most of them deal with fire detection and make use of temperature and humidity sensors, smoke detectors and infrared cameras. In (Chen, 2003) a fire-detection system is proposed based on multi-sensor technology and neural networks. The sensed contextual data includes environmental temperature, smoke density and CO density. In (Pehrsson, 2000) and (Pehrsson, 2003), the authors present a system that is based on various types of sensors and use neural networks. However such systems require the use of training data and most of them are evaluated indoors where the weather conditions are fully controllable and, surely, completely different in comparison with those observed in a WUI. A system for wildfire monitoring using a wireless sensor network (WSN) that collects temperature, relative humidity and barometric pressure is described in (Doolin, 2005). The authors in (Calle, 2006) and (Sivathanu, 1996) propose systems based on infrared (IR) technology for the detection of fires. Furthermore, (Kucuk, 2008) and (Kosucu, 2009) have proposed solutions in which sensors are deployed from an aircraft. In (Hefeeda, 2007) the authors propose a distributed k-coverage algorithm to balance the load across all deployed sensor nodes. However, these systems use either in-field or out-field sensors, thus rendering them vulnerable to false alarms. In addition, aerial or satellite images are frequently used for outdoor fire detection and monitoring. In (Mandel, 2007) the authors present a system architecture which attempts

Figure 1. SCIER system architecture

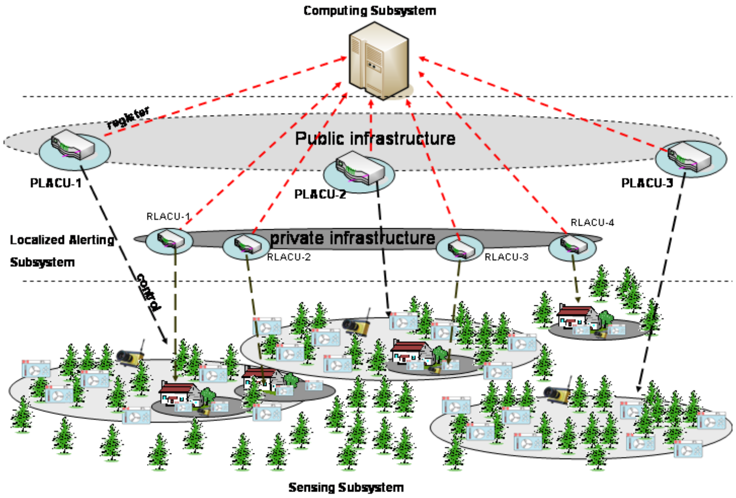

to integrate recent sensing measurements (from satellite spectral image data and other sensors) with simulation based predictive modelling into a closed loop system. The sensor data are used to calibrate the predictions of the simulation model in order to minimize the evolution prediction error. These methods are known as Dynamic Data Driven Application System (DDDAS) techniques and are recently of great interest to the scientific community. Satellite based monitoring is used for detecting forest fires in (Zhanqing, 2001). However, the scan period and the low resolution of satellite images make such method incapable for early (real-time) fire detection.

SCIER System

The SCIER platform is a complex system which integrates technologies and techniques from different scientific fields. It is customary that the architecture of such a large-scale integrated system is visualized by a vertical, bi-directional flow-chart divided into different layers. Each layer performs a specific set of activities. Neighboring layers contribute to their common interface so that all bilateral transactions are reliable and safe. In the SCIER case, we identify three (3) architectural layers: the Sensing Subsystem, the Localized Alerting Subsystem and the Computing Subsystem.

Sensing Subsystem

The purpose of the SCIER sensing subsystem is the monitoring of the environmental parameters that are relevant to the assessment of a natural hazard. In the WUI two kinds of sensors are deployed: Citizen Owned Sensors (COS), installed by land/home owners in fixed and registered locations in private areas, and Publicly Owned Sensors (POS), installed by state authorities in fixed and known locations in public areas. The sensor nodes (Figure 2) are energy efficient and form a multi-hop,

Figure 2. Sensor nodes used in SCIER system

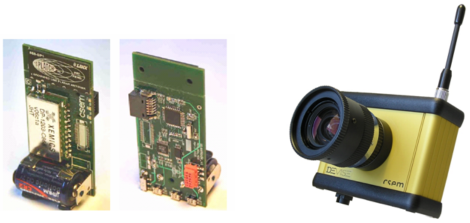

Figure 3. Distribution of the nodes on the field

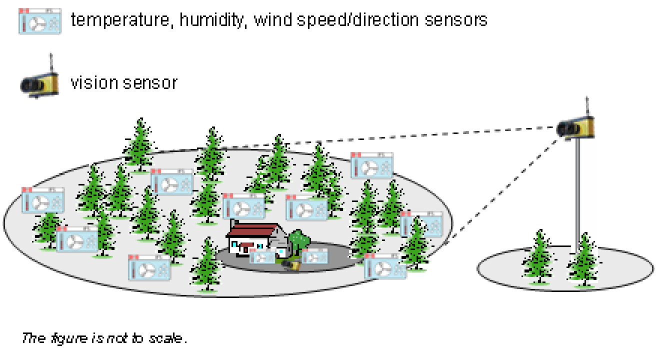
temperature, humidity, wind speed/direction sensors
vision sensor
The figure is not to scale.

self-organized, robust Wireless Sensor Network transmitting the raw measurements to a sink node via appropriate routing protocols. They are enclosed in appropriately designed (temperature and water resistant) plastic boxes which isolate them from the environment but do not affect the radio propagation. Outside the box is only the actual sensor (sensing part).The transmission range of the nodes is adjustable and can reach up to 250 m in open space areas and up to 100 m in a forest zone.

In SCIER the following categories of nodes are identified.

- **In-field sensor nodes.** They carry two or three sensors, and they are responsible for measuring and transmitting values of meteorological parameters (e.g., temperature and humidity). Since they are battery-powered, these nodes have high energy-consumption constraints. They transmit their readings towards the data sinks, following the multi-hop organization of the WSN. The WSN can be dynamically deployed which means that nodes can be added or removed at run-time according to the circumstances.
- **In-field sensor nodes - cluster heads.** They are similar to the sensor nodes except that they are more powerful and can support more complex sensors (e.g. wind measurements) as well. They propagate the information to the data sinks.
- **Out-of-field vision sensors ("smart cameras").** They report data from the scene under surveillance.
- **Data sinks.** They relay the information from/to the sensor nodes towards/from the SCIER's higher layers.

The use of out-field vision sensors that monitor the same area adds an extra feature to the system which contributes to the effective detection of a hazardous natural phenomenon. Vision sensors, in the case of a fire, transmit information about smoke or flame probability corresponding to locations on which the camera focuses and which are different from the location of the vision sensor. They provide a very stable representation of the scene under uncontrolled illumination conditions. Vision sensor nodes are fixed nodes, most likely installed on poles or citizens' homes. A monitored area could be covered by one or more vision sensors. Figure 3 depicts the distribution of the nodes on the monitored field.

Localized Alerting Subsystem

The Localized Alerting Subsystem (LAS) includes the Local Alerting Control Unit (LACU) which comprises a computing element of primary importance to the SCIER system. Each LACU controls

Figure 4. The Localized Alerting Subsystem of SCIER

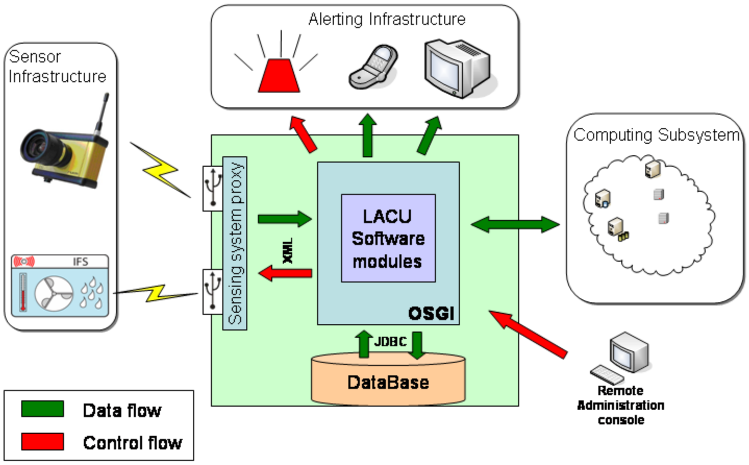

a network of sensors, receives input from them, and executes fusion algorithms on the received data. Multiple LACUs are deployed in the area that needs to be monitored for potential emergency situations arising from environmental hazards, such as forest fires or floods. Using LACUs can be extended to handling different environmental risks by adjusting the type of sensors and fusion algorithms used. The LACUs self organize into a network, where each node (a LACU) has certain functional autonomy, but can also be controlled by the Computing Subsystem, in certain cases. In SCIER, two types of LACUs are identified (Figure 1):

- Public LACU (P-LACU). It is installed and operated by public authorities and controls a wireless network of Public Owned Sensors.
- PRivate LACU (R-LACU). It controls Citizen Owned Sensors and is installed by individuals in order to protect their private properties.

The LACU is a device which mediates between the Computing Subsystem and the Sensing Subsystem. It is a simple computing unit, which runs specific software developed in the context of the SCIER project. This software is based on the OSGI framework (OSGI Alliance, 2009) and is highly modular enabling to load/unload or update components on demand. The basic software components comprising LACU (Figure 4) have the following roles:

- Control of the WSN
- Acquisition of data from the underlying WSN. Currently supported sensors include temperature, humidity, wind speed & direction sensors, pluviometers and vision sensors assessing smoke and flame probability
- Administration of the system, which can be performed either locally or remotely
- Execution of flood/fire detection algorithms that assess the severity of the readings flowing in the system and produce alerts
- Support for various alerting components (visible, acoustic, SMS messaging) used to provide notifications when potential emergencies are detected
- Communication with external computing elements (i.e., the Computing Subsystem)

Computing Subsystem

The Computing Subsystem (CS) is largely based on a GIS where the fused sensor information is stored, processed and visualized. Multiple environmental models of different time scales are used in order to establish an accurate tracking (and simulation) of the hazardous phenomenon. The risk models are executed in the CS, providing estimates on the spreading of the risk and the expected impact and arrival time for settlements, villages and farms. Advanced computing infrastructure (e.g., a Grid setup) can be used to run "what-if" scenarios, thus investigating the consequences of potential changes in key environmental parameters such as the wind speed and direction. The Grid infrastructure offers the capability of parallel simulations which allow the exploration of the effects of potential changes in such parameters.

The main functionalities of Computing Subsystem are:

- Collect and store sensor-measurements from the area of interest.
- Perform data-fusion-algorithms to assess the level of risk.
- Trigger a simulation in case of a perceived real alarm, i.e. (a) retrieve geographical data from the GIS Database on the terrain layout of the area of interest, (b) generate different slightly perturbed scenarios on the wind speed and wind direction for the area of interest, (c) submit to the Grid parallel simulations, one for each scenario, (d) retrieve results and pass them to the GIS module for visualization on a reference map

Fusion Process in SCIER

In SCIER, as discussed in previous sections, data derived from various sensors are used for the detection and monitoring of hazardous events. Such sensors include temperature, humidity, wind speed/direction, pluviometry, soil moisture and vision sensors. The volume of raw data that are generated requires an effective post-processing in order to decide on the occurrence (or not) of an event. Thus, sensor fusion techniques which process and assess the data and reason about an event are adopted.

In the case of fire detection one requires measurements derived from in-field sensors that are deployed in the area or out-field sensors which monitor from a distance the area. In the SCIER system temperature, humidity sensors (in-field) and vision sensors (out-field) are used. The last are based on a high-dynamic range contrast camera in which the contrast representation of a scene can be used (through appropriate algorithms) to detect smoke or flames and estimate/generate a probability (confidence level) on this event. These two categories of sensors are combined in a two-level fusion scheme (Zervas, 2009), (Zervas, 2007) thus improving the reliability of the system in fire detection. At the first level of fusion (data fusion) we adopt the cumulative sum technique (Gombay, 2005), (Page, 1954) for fusing data from in-field sensors and assign a probability of fire occurrence in each of them. At the second level fusion (information fusion), probability values about fire events from the first level are combined through evidential theory with probability values about fire events from the vision sensor. The adoption of such a scheme has the advantage of early fire detection and, simultaneously, eliminates any false alarms in case of no fire occurrence. Figure 5 depicts the whole work flow regarding the aspect of the fusion process (data and information) in SCIER.

First Level Fusion

In each LACU readings from in-field sensors are constantly processed through a sensor data fusion procedure in order to detect any significant change in the environmental state. For instance, consider the event in which the normal ambient

Figure 5. Fusion process in SCIER

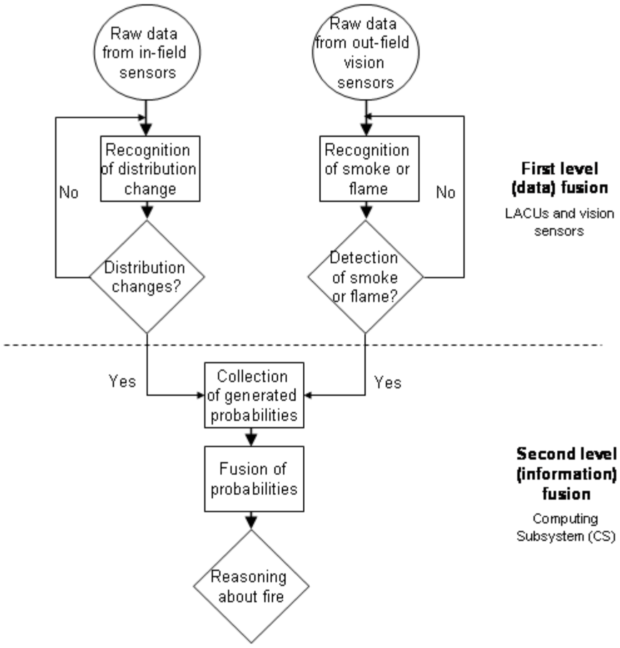
Raw data from in-field sensors
Raw data from out-field vision sensors
Recognition of distribution change
Recognition of smoke or flame
No
No
Distribution changes?
Detection of smoke or flame?
First level (data) fusion
LACUs and vision sensors
Yes
Yes
Collection of generated probabilities
Fusion of probabilities
Second level (information) fusion
Computing Subsystem (CS)
Reasoning about fire

temperature increases in an abnormal way. This could indicate the occurrence of a possible fire event. The system regularly monitors the data distribution that is generated over time. If a change in data distribution is detected, this is reflected on a specific “metric”. Such “metric” postulates a translation of the impact of the evidence to a certain amount of belief on a current hypothesis (the fire event hypothesis in our case). Such probability is calculated for each sensor.

In an analogous data fusion procedure, for each out-field vision sensor, any significant change in the contrast or the luminance of the monitored scene is translated, through specific algorithms, to a probability of fire (smoke or flame). According to the luminance of the environment which depends on the time of the day the vision sensor which divides the scene into tiles, generates the appropriate probability for each tile. Smoke probability in the daylight and flame probability at night. Each sensor *Si* (temperature, humidity, vision sensor) produces a confidence level c_i for fire detection in its monitoring area and reports this value to the Computing Subsystem (CS) where the second level fusion takes place. The confidence levels indicate an order in probability of positive detection in the sense that a higher confidence level implies a higher probability of fire.

Second Level Fusion

In the second level fusion process vision sensor (camera) data and data coming from LACUs are combined. Each single fusion process will be based on data for a single camera tile together with data from the sensors that this camera tile oversees. In those cases where a camera tile does not oversee any sensor(s), or a/any sensor(s) is/are not overseen by a camera, a degenerate fusion process will be carried out taking into account the probabilities of a single camera tile or any sensor(s) respectively.

Upon reception of the confidence levels c_i, i=1,…,M the fusion process at CS evaluates a discriminant function f(c_1, c_2, c_3 …,c_M) and compares it with a threshold t, to decide if a fire

Figure 6. Second level fusion in SCIER

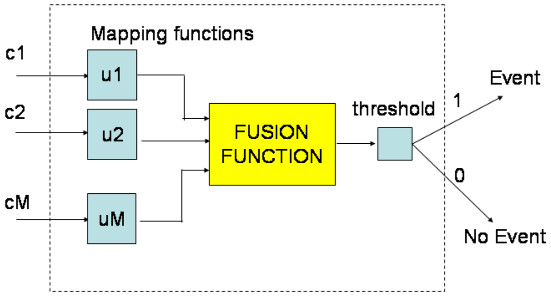

event is present or not. The fusion methods may treat the influence of the confidence levels differently and this is shown schematically in Figure 6 where mapping functions are used to scale the confidence levels.

Confidence levels are combined through Dempster–Shafer (DS) evidential theory (Shafer, 1976). In DS process for each sensor we need the basic probability assignments $m(F)$, $m(no - F)$ and the unsigned probability mass $m(F\ U\ no - F)$. These quantities sum to one, thus only two of them need to be specified. The mass $m(F)$ represents the belief in fire detection, $m(no - F)$ the belief in the no–fire case and $m(F\ U\ no - F)$ represents the uncertainty of the sensor. Given the confidence level of a sensor, c_i, and the uncertainty u_i, the mapping function can be:

$$m_i(F) = (1 - u_i)c_i$$
$$m_i(noF) = (1 - u_i)(1 - c_i)$$
$$m_i(F \cup no - F) = u_i$$

The Dempster – Shafer algorithm for fusing two probability masses is

$$m_{12}(F) = \frac{1}{1-K}[m_1(F)m_2(F) + m_1(F)m_2(F \cup no - F) \\ + m_1(F \cup no - F)m_2(F)]$$

$$m_{12}(no - F) = \frac{1}{1-K}[m_1(no - F)m_2(no - F) \\ + m_1(no - F)m_2(F \cup no - F) \\ - m_1(F \cup no - F)m_2(no - F)]$$

$$m_{12}(F \cup no - F) = \frac{1}{1-K}[m_1(F \cup no - F)m_2(F \cup no - F)]$$

where

$$K = m_1(F)m_2(no - F) + m_1(no - F)m_2(F)$$

For fusing the probabilities of three sensors, one has first to combine two sensors to obtain $m_{12}(F)$, $m_{12}(no - F)$ and $m_{12}(F\ U\ no - F)$ and then use Dempster-Shafer rule to obtain $m_{123}(F)$, $m_{123}(no - F)$ and $m_{123}(F\ U\ no - F)$. Once exhausting the sensors we are left with the basic probability masses:

$m_{123\cdots M}(F)$, $m_{123\cdots M}(noF)$ *and* $m_{123\cdots M}(F\ U\ no - F)$

For detection purposes we can use either the support $m_{123\cdots M}(F)$ and compare it to a threshold t, or the plausibility $m_{123\cdots M}(F) + m_{123\cdots M}(F\ U\ no - F)$ and compare it to a threshold t, or even the average of these two.

Examples of the Fusion Process

Scenario 1. In this scenario we combine the maximum probability induced by the in-field sensors (in order to minimize the false alarm rate) with the fire detection probability of the vision sensor. We assume three different fire probabilities for the vision sensor (0.1, 0.5, 0,9), each one fused with three different probabilities (0.1, 0.5, 0.8), inferred by the LACU using in-field sensor measurements. Table 1 shows the combination results of the DS algorithm. As it is observed, unless both fused probabilities exceed the value

Table 1. DS algorithm on fusing the probability regarding the fire event of an in-field sensor with the vision sensor

In field Sensor 1 $m_1(F)$	Vision Sensor $m_2(F)$	Conflict (K)	Fused Probabilities $m_{12}(F)$ In field Sensor 1 + Vision Sensor
0.1	0.1	0.18	0.0122
0.1	0.5	0.50	0.1000
0.1	0.9	0.82	0.5000
0.5	0.1	0.50	0.1000
0.5	0.5	0.50	0.5000
0.5	0.9	0.50	0.9000
0.8	0.1	0.74	0.3077
0.8	0.5	0.50	0.8000
0.8	0.9	0.26	0.9730

of 0.5, the final probability is kept in relatively small values. Thus, a malfunctioning sensor is not able by itself to trigger a fire alarm. Moreover high probability values of both sensors will enhance our confidence for a fire event.

Scenario 2. In this scenario we combine the fused probabilities obtained in the first scenario with the fire detection probability of another in-field sensor (Sensor 3). For the latter, we assume two values (0.2 and 0.6) and the results are depicted in Table 2 and Table 3 respectively. As it is observed from the entries of Table 2 (rows 3 and 5), the value 0.5 when combined with the small probability of the in-field sensor i.e., 0.2, yields the lowest value, that is 0.2.

On the contrary, as it is observed from Table 3 (rows 3 and 5), the value 0.5 when fused with a higher probability, i.e., 0.6, yields the maximum value, that is 0.6. If all constituent probabilities are greater than 0.5 (last two rows of Table 3) then our belief for a fire event is reinforced as it is indicated by the high values of the final fused probability.

Table 2. DS fusion algorithm with a second in-field sensor (probability 0.2)

Fused Probabilities $m_{12}(F)$ In field Sensor 1 + Vision Sensor	In field Sensor 3 $m_3(F)$	Conflict (K)	Fused Probabilities $m_{123}(F)$
0.0122	0.2	0.2073	0.0031
0.1000	0.2	0.2600	0.0270
0.5000	0.2	0.5000	0.2000
0.1000	0.2	0.2600	0.0270
0.5000	0.2	0.5000	0.6000
0.9000	0.2	0.7400	0.6923
0.3077	0.2	0.3846	0.1000
0.8000	0.2	0.6800	0.5000
0.9730	0.2	0.7837	0.9000

Table 3. DS fusion algorithm with a second in-field sensor (probability 0.6)

Fused Probabilities m_{12}(F) In field Sensor 1 + Vision Sensor	In field Sensor 3 m_3(F)	Conflict (K)	Fused Probabilities m_{123}(F)
0.0122	0.6	0.5975	0.0182
0.1000	0.6	0.5800	0.1429
0.5000	0.6	0.5000	0.6000
0.1000	0.6	0.5800	0.1429
0.5000	0.6	0.5000	0.6000
0.9000	0.6	0.4200	0.9310
0.3077	0.6	0.5384	0.4000
0.8000	0.6	0.4400	0.8571

FIRE FRONT EVOLUTION SIMULATION - GRID WORKFLOW

The fusion algorithms, described in the previous section, decide whether the event constitutes a real threat or it is a false alarm. In the former case the SCIER Computing Subsystem initiates a simulation in the Grid infrastructure consisting of several parallel runs. Each run is based on a different set of input parameters and computes:

- The expected evolution of the fireline for up to 180 minutes after fire detection. The Fire Spread Engine (FSE) software program developed by Technoma S.A. (EUFIRELAB, 2006) is used for this purpose. The FSE is a computer application which estimates the fire front expansion on surface forest fuels, using spatial data about the topography, moisture content, type of the fuel and dynamic environmental parameters, such as the wind vector field. The software is based on the Rothermel-Frandsen theoretical model and uses algorithms similar to those found in the BEHAVE system (Andrews, 1986). A cellular-automata algorithm is used for the estimation of the fire spread. However, the major limitation of all fire spread simulators (including the FSE) is that their accuracy decreases as the span of the prediction time increases. An acceptable prediction time span for the FSE is usually up to 2-3 hours after fire detection.
- In addition to the fire front line, a simulation run also estimates the time-evolving temperature field it induces as it moves through an area. For that purpose we use the *Temperature Field Modeling* (TFM) software component that we have developed (Manolakos, 2008).

At the end of a simulation, the different temperature fields estimated by the parallel TFM components are compared to the real temperature field measured at the deployed sensor locations in order to infer the posterior probabilities of the different simulated fire front scenarios given the real sensor data. Algorithms for matching (real to hypothesized scenarios) and scoring scenarios probabilistic similarity have been developed for this purpose. The larger the number *N* of simulated fire front evolution scenarios, the more accurate the estimated posterior probabilities of the scenarios given (sufficient data collected from) the real event. Since fire spread is a very complex phenomenon influenced by many diverse factors, one can hope to estimate accurately the probability

Figure 7. Components of the SCIER forest fire simulation workflow. Most components run inside the Grid. The matching and scoring components currently are not GRIDified.

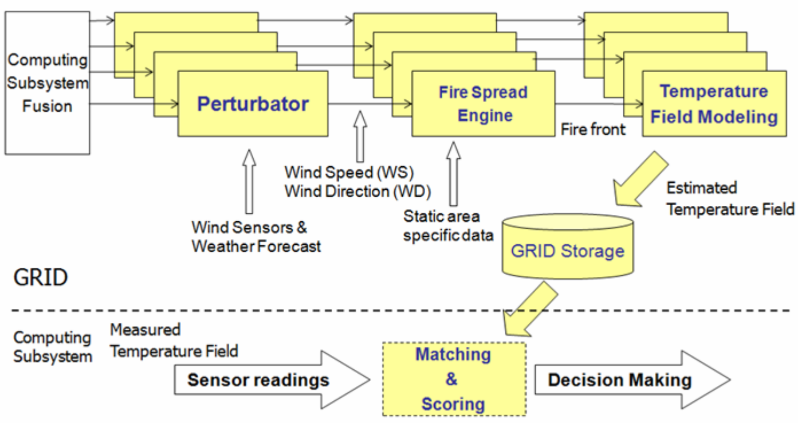
Computing Subsystem Fusion
Perturbator
Fire Spread Engine
Temperature Field Modeling
Fire front
Wind Speed (WS)
Wind Direction (WD)
Wind Sensors & Weather Forecast
Static area specific data
Estimated Temperature Field
GRID Storage
GRID
Computing Subsystem
Measured Temperature Field
Sensor readings
Matching & Scoring
Decision Making

of arrival of a fire line to a specific area only if an effective sampling mechanism of the very large parameter space is in place (Bianchini, 2005). The parallel processing capabilities provided by the Grid infrastructure, help us complete the simulation of a large number of alternative scenarios in a reasonable amount of time, compared to a serial execution.

The workflow of a wildfire evolution simulation includes a set of components whose interaction is shown in Figure 7. The workflow starts with the generation of the different wind speed and direction fire scenarios to be simulated. This is the task of a component called the "Perturbator". The *Perturbator* uses current wind sensor measurements and wind weather forecasts for the next few hours to estimate the mean and extend of wind parameters and then produces, by random sampling from a statistical distribution (Gaussian or uniform), a wind speed and wind direction combination (WS, WD) to be simulated.

A wind scenario ((speed and direction combination generated by the Perturbator) is supplied as input to an FSE component instance which estimates the corresponding fire front's spatio-temporal evolution for the next 180 min. The number of simulated scenarios depends on the number of different wind speed and direction combination pairs (WS, WD) generated and is a user controllable parameter. Each scenario corresponds to a simulation run and all the runs included in the same simulation job are executed in parallel in the Grid. In addition to the wind speed and direction dynamic data, the FSE needs as input data files related to the ground morphology (slope, aspect), moisture, fuel type etc. These files are specific to a geographic area of interest, do not change from run to run (static data) and need to be available before a Grid simulation can be launched.

The execution of an FSE component instance generates the data needed to launch subsequently a *Temperature Field Modeling* (TFM) component instance (Manatakis, 2010, Manolakos 2008). This component takes as input the output files produced by the FSE (time of arrival of the fire line at each geographical cell, fire flame length at time of arrival) and the corresponding wind speed and direction files and produces *in-silico* an estimate of the temperatures that the in-field temperature sensors located close to the fire front line are expected to "feel". Temperature estimates are updated every time the front line is advanced, i.e. every minute. Therefore, if a simulation includes *N* (WS,WD) runs, these will simulate in parallel *N* different fire front line evolution scenarios and produce their respective *N* temperature fields. If

Figure 8. Fire front evolution estimation

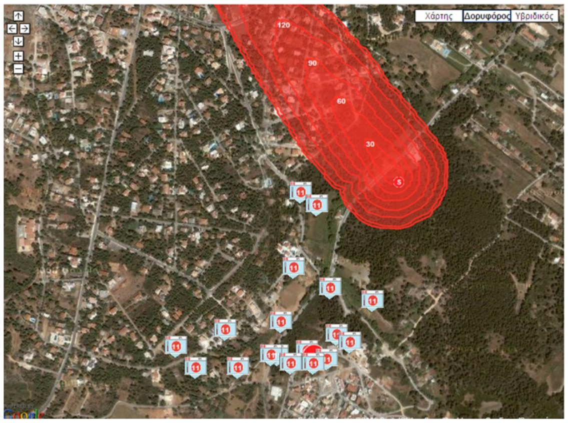

the FSE is simulated say for 180 minutes, then the corresponding temperature field produced by the TFM component basically corresponds to a “thermal video” with 180 successive “temperature frames” and as many pixels per frame as the deployed SCIER sensors in the field. The TFM component is the most computationally demanding in the Grid workflow. At each simulation time step its time complexity increases with the product of the number of cells newly affected by the fire and the number of sensors (monitoring points) existing close to the fire front line.

To rank order the simulated scenarios in terms of how probable they are, we compare periodically the temperature fields, estimated in-silico by the different Grid TFM runs, to the set of real sensor measurements (temperature readings) as they become available from the SCIER sensing subsystem after the confirmation of a true fire event. The process that assesses the degree of similarity of the real temperature sensor data to the in-silico produced temperature estimates is called field *matching*. It is followed by the *scoring* process which estimates how probable is each one of the simulated fire front evolution scenarios based on the results of the matching and in light of the already collected sensor measurements. Scoring also produces a map that shows the probability that each geographical cell will be affected by the fire for the next up to 180 minutes after fire detection. This may be estimated using either all N simulated scenarios or the $M < N$ most probable ones identified by the scoring process. The matching and scoring processes can be iterated periodically to improve the scoring accuracy by exploiting more WSN collected temperature data, as they become increasingly available from the SCIER sensing subsystem as the fire progresses. The matching and scoring SCIER software components run outside the Grid (in the CS server) because their computational time is not substantial. However if N becomes very large, a Grid implementation may also be considered for their implementation. The visualization of a typical scenario regarding the fire front evolution is depicted in Figure 8.

RESULTS AND DISCUSSION

To evaluate the efficiency of the proposed GRID computing workflow, we have performed extensive simulations with different numbers of runs (ranging from 5 to 110). Each run corresponds to a specific forest fire scenario which simulates 180 min of fire front evolution and temperature field generation for a fire that is started at a specific ignition point in the area of Stamata, a WUI community outside Athens, Greece. Stamata has been selected as one of the SCIER project field trial areas and a WSN with 20 temperature sensor nodes and 2 vision sensors has been deployed in order to be able to test and evaluate the overall SCIER system’s behavior and performance under real world conditions during the summer period, when the risk for fire events occurring is higher. All the simulated fire front evolution scenarios run in one of the sites of the national GRID infrastructure, where P=40 CPU slots (*specint*2000=1367) have been reserved for SCIER simulations. The adopted middleware used was *glite* version 3.0 (Hellas Grid, 2008).

Figure 9. (a) Burned area (in hectares), under different wind speed and wind direction conditions (b) Number of runs completed at each time step (min) of the grid execution time.

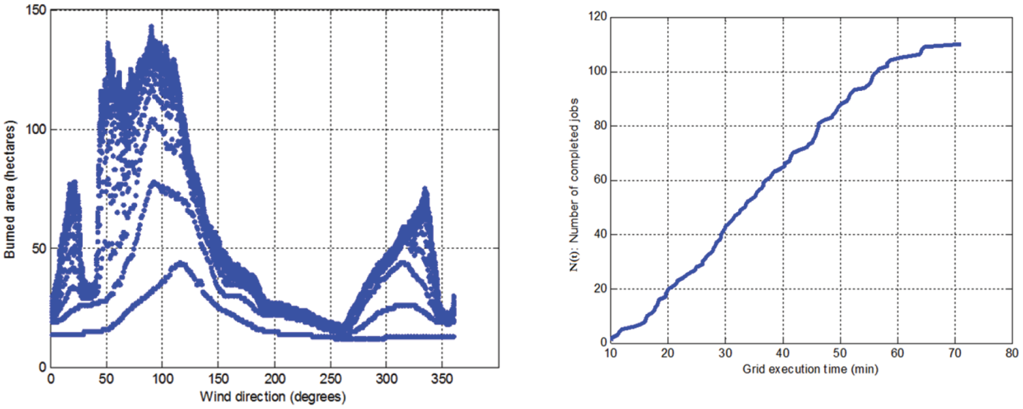

(a)

(b)

Simulation Setup

For the FSE component to work the area of Stamata has been organized as a geographical grid with 501x501 square "cells", each cell having a side of 6 m. The static input files (produced by field experts using GIS systems and data bases) provide to the FSE information about the ground morphology (slope, aspect), the fuel type and fuel moisture (dead and live) which dominates at each cell.

In order to simulate a fire spread evolution scenario, apart from the aforementioned static input files, the FSE needs information about the prevailing wind speed and direction conditions. Running the FSE with different wind speed and direction input parameters provides us with different fire front evolutions scenarios. In Figure 9(a) we observe for a given wind direction, the dependence of the burned area (in hectares) on the different wind speeds is ranging from 1 m/sec to 42 m/sec. Since the execution times of the FSE and TFM components depend on the burned area, which may vary greatly with the wind speed and direction for the same geographical area and ignition points, we cannot predict a priori the execution time of a simulation run.

For the simulation experiments whose results are reported here, the Perturbator component used as current wind speed and direction the values 10 m/sec, 270 degrees and as weather forecasted values 20 m/sec, 360 degrees respectively. To generate different wind speed and wind direction scenarios the Perturbator sampled a normal distribution with mean value the mid-range and standard deviation the half-difference between forecasted and current values. The number of deployed sensors, whose temperature vs. time curves have to be estimated by the TFM component for each scenario, was 20 matching the number of sensors which have actually been deployed in the Stamata test site.

Evaluation Method

Let $N(t)$ denote the number of parallel runs included in a simulation that have been completed in the Grid by time t (min) after the simulation's initiation. Let $T_s(t)$ be the aggregate serial execution time of all these runs if they were to be executed serially (the one after the other) in a single Grid worker node. Let $T_q(t)$ be the aggregate Grid overhead time spent collectively by all the $N(t)$ runs in scheduling queues and other non-execution Grid stages. Let $S(t)$ denote the *speedup* factor

Figure 10. (a) Solid and dotted curves show the aggregate serial computational time Ts(t) and the aggregate time in queue Tq(t) respectively. (b) Computational speedup using the Grid.

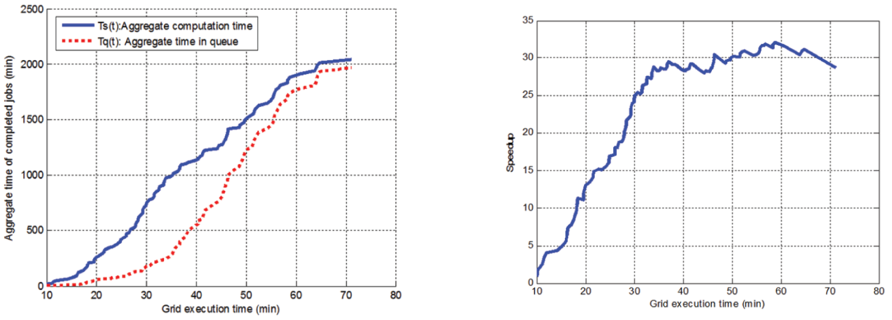

(a)

(b)

which has been realized using the Grid by time t. It can be computed as $S(t) = T_s(t) / t$. Finally let $E(t)$ denote the grid running *efficiency,* measuring deviation from the ideal linear speedup at time t and computed as $E(t) = S(t) / p$, where p is the number of slots allocated to the execution of the $N(t)$ parallel runs.

Experimental Results and Discussion

The experimental results presented next correspond to a simulation consisting of 110 runs (i.e. sumulating 110 different fire front evolution scenarios) executed using 40 reserved CPU slots provided by a single HellasGrid site (Hellas Grid, 2008). Figure 9(b) shows the number of completed $N(t)$ jobs as a function of parallel grid time t. We observe that it takes 71 min to complete all 110 jobs, i.e. the effective grid throughput is approximately ~1.54 jobs/min, as opposed to ~0.054 job/min in a single worker node machine.

Figure10(a) shows two curves, the solid and dotted curves correspond to the aggregate computation time $T_s(t)$ and the aggregate scheduling and in-queue time $T_q(t)$ respectively, of all the runs completed by time t. As time progresses, we observe that the aggregate time spent by all completed runs collectively in the queue increases (as expected) and tends to reach the aggregate serial time of the runs. Two factors contribute to the rate (slope) of $T_q(t)$, one is the rate of the number of completed jobs $N(t)$ (shown in Figure9(b)) and the other is the time the corresponding jobs spent waiting in the queue. For $t < 30$ min, the rate of $T_q(t)$ is lower as this part of the curve corresponds to the first bunch of jobs that are scheduled to CPU slots immediately and therefore spend minimum time in the queue. Also, as shown in Figure 9(b), the rate of $N(t)$ for t>60 min decreases, which explains the decrease of the rate of $T_q(t)$, as at this phase the rate of $N(t)$ becomes the dominating factor. Figure 10(b) shows the grid realizable speedup as grid execution time increases. We observe that when the number of parallel runs exceeds the number of available CPU spots the speedup factor levels off, but is sustained at ~30 which is a very respectable steady state value considering that we are using $p=40$ CPU slots i.e. the maximum theoretical speedup is equal to 40. This indicates that for a large number of runs (scenarios) parallel computation can be very efficient, exceeding the 75% efficiency level.

EXPLOITATION

The definition of the spatial scale and the main protected entity will be the cornerstone for the design and execution of a strategy towards the exploitation of the SCIER system. The main objective of the SCIER system implemented in a protection cell (a settlement, a small housing area, a small town) is to obtain data from that cell, monitor the evolution of fire, offer better protection, and perform more effective deployment of forces in the affected areas.

The product to be designed as marketable should be based on what has been developed in the project, namely network of wireless sensors, prediction models, spatial data processing and communication technologies. It should follow a scalable and inter-operable approach, in this way the initial deployment of the SCIER components will serve as a system seed around which new nodes can be added to the initial protection cell. New cells can be aggregated to support co-operative monitoring among settlements meening that the sensors of remote cells can be used locally, thus extending the power and efficiency of all sensors deployed in the area. The design of the system should count on private homeowners or industrial installations, that may also request more specific and dense network of sensors for their own purposes, but that can be used within the network to protect other properties and infrastructures as well. For the definition of the concept, a protection cell will include also a buffer zone (e.g. 0.5 km) and, depending on the pattern and density of houses/vegetation, other buffer areas inside the settlement where sensors should be deployed. Experience shows that, in case of WUI detected fires, the protection should focus mainly on the first ring of houses that are normally more exposed to the incoming risk.

The SCIER system can be adopted by local authorities like municipalities and prefectures for the protection of varying scales of land against fires. Such authorities are strongly interested in detecting incidents at the earliest possible time and issue early warning alarms to the people living in their areas of responsibility. The IT personnel of municipalities/prefectures deploys the system at designated areas of high risk and assumes the responsibility for its maintenance. Moreover, such a public system may interoperate with private SCIER systems in a collaborative way in order to extend system's coverage and optimize its operation. Moreover, the vast sensor feed accumulated in the SCIER system and the local danger assessment could be of vital importance to central government emergency services, such as the Civil Protection Authority. Such authority should obtain accurate information on the development of hazardous phenomena and centrally orchestrate the risk management tasks (e.g., allocate fire fighting units, dispatch ambulances etc).

FUTURE WORK

As a future work, we propose the enhancement of the implemented fusion algorithms with alternative combination rules, e.g., (Yager. 1987) and the adoption of the Fuzzy Set theory to deal with uncertainty, imprecision and incompleteness of the underlying data. Further validation through trials with controlled flaming or smoldering fire should be conducted to quantify parameters such as thresholds, false alarm rates and fusion weights. As mentioned in previous sections, 40 CPU slots have been reserved for SCIER purposes in the GRID infrastructure, therefore the waiting time of a simulation job is more predictable. However, considering that SCIER jobs are triggered rarely but unexpectedly by non-periodic events and that sustained CPU reservations may not be practical in large-scale deployments, we are investigating novel grid resources scheduling models that could provide a viable alternative. In addition to the notion of grid CPU slots, which typically have a one to one correspondence with the operating system CPU slots of the worker nodes, this model introduces to grid middleware the concept of *virtual* grid CPU slots. Virtual grid CPU slots are made available only to specific job types with soft real time requirements and short deadlines. According to this model SCIER jobs will be neither delayed due to other jobs nor queued while waiting for a grid CPU slots to be released.

CONCLUSION

In this chapter we have presented the SCIER system which focuses on the detection and monitoring of environmental risks. In its current form, the SCIER system/architecture can deal with forest fires and flash floods, with emphasis on the protection of the WUI areas. Throughout the chapter, we elaborated on the fire hazard case. Detection of fires in SCIER is performed through a multi-sensor infrastructure integrating wind-speed, wind-direction, temperature, humidity and smart vision sensors. To cope with all these different types of sensors and deliver alarms with increased accuracy and confidence a layered fusion scheme has been adopted. Different sensor feeds are processed in the two layers of the fusion scheme. On the lower layer, the statistical behavior of sensor data is constantly assessed. On the higher layer, D-S theory of evidence is adopted in order to mix the indications coming from the lower layer and the out-of-field vision sensors. We provide examples to clearly illustrate the adopted scheme. Apart from the SCIER fusion model, we also discuss the advanced simulation architecture developed in the context of the project. Specifically, we have developed an end-to-end grid workflow which involves the parallel execution of many alternative fire evolution scenarios. The workflow has been evaluated in the area of Stamata, Greece. The analysis of our experimental results demonstrates the potential speedup that can be delivered by the grid infrastructure to the application. Parallel simulations allow the investigation of the effects of perturbations in critical environmental variables and the joint assessment of probabilistic scenarios to derive meaningful predictions and corresponding crisis management plans before the disaster strikes.

REFERENCES

Andrews, P. L. (1986). *BEHAVE: fire behavior prediction and fuel modeling system- BURN subsystem. Part 1. GTR-INT-194*. USDA Forest Service.

Bianchini, G., Cortés, A., Margalef, T., & Luque, E. (2005). S2F2M - Statistical System for Forest Fire Management, Atlanta, USA. In P*roceedings of the Int. Conf. on Computational Science*, ICCS Book of Abstracts.

Calle, A., Casanova, J. L., & Romo, A. (2006). Fire Detection and Monitoring using MSG Spinning Enhanced Visible and Infrared Imager (SEVIRI) Data. *Journal of Geophysical Research*, *111*, G04S06. doi:10.1029/2005JG000116

Chen, S., Bao, H., Zeng, X., & Yang, Y. (2003). A Fire Detecting Method based on multi-sensor Data Fusion. In IEEE Systems Man and Cybernetics, 4.

Deliverable, E. U. F. I. R. E. L. A. B. D-03-06. (n.d.). Retrieved September 9, 2008, from http://www.eufirelab.org

Doolin, D. M., & Sitar, N. (2005). *5765*. Wireless Sensors for Wildfire Monitoring. In Smart Structures and Materials.

Gombay, E., & Serban, D. (2005). An adaptation of Pages CUSUM test for change detection. *Periodica Mathematica Hungarica*, *50*, 135–147. doi:10.1007/s10998-005-0007-7

Hefeeda, M., & Bagheri, M. (2007). Wireless Sensor Networks for Early Detection of Forest Fires. Pisa, Italy. In *Proceedings of the 1st International Workshop on Mobile Ad hoc and Sensor Systems for Global and Homeland Security (MASS-GHS)*, Pisa, Italy.

Hellas Grid. (n.d.). Retrieved September 10, 2008, from www.hellasgrid.gr.

Kosucu, B., Irgan, K., Kucuk, G., & Baydere, S. (2009). FireSenseTB: A Wireless Sensor Networks TestBed for Forest Fire Detection. In the *5th ACM International Wireless Communications and Mobile Computing Conference (IWCMC'09), Leipzig, Germany*.

Kucuk, G., Kosucu, B., Yavas, A., & Baydere, S. (2008). FireSense: Forest Fire Prediction and Detection System using Wireless Sensor Networks. In the *4th IEEE/ACM International Conference on Distributed Computing in Sensor Systems (DCOSS'08), Santorini Island, Greece*.

Manatakis, D. V., Manolakos, E. S., Xanthopoulos, G., Roussos, A., & Viegas, D. (2010). In-silico estimation of the temperature field induced by a moving fire – Predictive modeling and validation using prescribed burn data. In the *VI International Conf. on Forest Fire Research*, Coimbra, Portugal.

Mandel, J., Beezley, J., Bennethum, L., Chakraborty, S., Coen, J., & Douglas, C. L, Hatcher, J., Kim, M., & Vodacek, A. (2007). A Dynamic Data Driven Wildland Fire Model. Computational Science - ICCS 2007 (pp. 1042-1049).

Manolakos, E. S., Manatakis, D., & Xanthopoulos, G. (2008). Temperature Field Modeling And Simulation of Wireless Sensor Network Behavior During a Spreading Wildfire, Lausanne – Switzerland. In *Proceedings of the European Signal Processing Conference*, EUSIPCO.

OSGi Alliance. (2009). http://www.osgi.org.

Page, E. S. (1954). Continuous Inspection Schemes. *Biometrika*, *41*, 100–115.

Rose-Pehrsson, S. L., & Hart, S, J., Street, T. T., Williams, F. W., Hammond, M. H., Gottuk, D. T., Wright, M. T., & Wong, J. T. (2003). Early warning fire detection system using a probabilistic neural network. *Fire Technology*, *39*(2), 147–171. doi:10.1023/A:1024260130050

Rose-Pehrsson, S. L., Shaffer, R. E., Hart, S. J., Williams, F. W., Gottuk, D. T., Strehlen, B. D., & Hill, S. A. (2000). Multi-criteria Fire Detection Systems Using a Probabilistic Neural network. *Sensors and Actuators. B, Chemical*, *69*(3), 325–335. doi:10.1016/S0925-4005(00)00481-0

Shafer, G. (1976). *A mathematical theory of evidence*. Princeton, NJ: Princeton Univ. Press.

Sivathanu, C., & Tseng, L. K. (1996). *Fire Detection Using Near-IR Radiation and Source Temperature Discrimination.* National Institute of Standards and Technology. Annual Conference on Fire Research.

Stewart, S. I., Radeloff, V. C., Hammer, R. B., & Hawbaker, T. J. (2007). Defining the Wildland Urban Interface. *Journal of Forestry*, *105*, 201–207.

Yager, R. R. (1987). On the Dempster-Shafer Framework and New Combination Rules. *Information Sciences*, *41*, 93–137. doi:10.1016/0020-0255(87)90007-7

Zervas, E., Mpimpoudis, A., Anagnostopoulos, C., Sekkas, O., & Hadjiefthymiades, S. (2009). *Multisensor Data Fusion for Fire Detection and Monitoring*. International Journal on Multi-Sensor, Multi-Source Information Fusion.

Zervas, E., Sekkas, O., Hadjiefthymiades, S., & Anagnostopoulos, C. (2007). Fire Detection in the Urban Rural Interface through Fusion techniques, Pisa, Italy. In *Proceedings of the 1st International Workshop on Mobile Ad hoc and Sensor Systems for Global and Homeland Security (MASS-GHS)*, Pisa, Italy.

Zhanqing, L., Khananian, A., Fraser, R., & Cihlar, J. (2001). *Automatic Detection of Fire Smoke using Artificial Neural Networks and Threshold Approaches applied to AVHRR Imagery*. IEEE Trans. On Geoscience and Remote Sensing.